Dual-Folding Based Rapid Search Method for Long PN-Code Acquisition

Hong Li, *Student Member, IEEE,* Xiaowei Cui, Mingquan Lu, and Zhenming Feng

***Abstract*—For long PN-code, rapid acquisition is difficult due to large search space. To speed up the search process, extended replica folding acquisition search technique (XFAST), which directly reduces the code phases to be searched by folding local signal, provides an efficient approach to rapid acquisition. Nevertheless, after folding the correlation properties of PN-code are degraded; hence, the detection performance of XFAST to weak signal is worse than that of nonfolding methods. To improve the detection performance, a dual-folding acquisition method (DF) is proposed. By folding both incoming signal and local signal, DF extends coherent integration time to enhance detection performance and indirectly reduce mean acquisition time. Numerical results demonstrate the enhancement of the proposed method with respect to other methods such as serial search (SS), zero-padding method (ZP), and XFAST.**

***Index Terms*—Code acquisition, dual-folding, correlation properties, detection performance, mean acquisition time.**

I. Introduction

SPREAD spectrum techniques have been widely applied in present day communication and navigation systems to overcome jamming or interception, or provide multiple access or ranging capabilities. A common derivation of spread spectrum is the direct sequence spread spectrum (DSSS) where the binary data sequences are multiplied by much higher rate pseudo-noise (PN) sequences before they are transmitted. Since long PN sequences can provide higher tolerance to jamming and spoofing than shorter ones [1], they are desirable in some fields such as military communication and navigation systems.

In the receiver, before demodulation of data sequences, the reception of DSSS signals requires a despreading processing, which can be performed in two steps. The first step is acquisition where the receiver and transmitter are synchronized within a certain uncertainty, typically within one PN-code chip interval. Then the second step of tracking, i.e., the fine synchronization between the transmitter and receiver, follows. If PN-code acquisition fails, communication or navigation is out of the question.

Due to the broad search space resulting from long PN-code, the acquisition requires elaborate work. Many methods have been addressed for this field [2]-[14]. Full parallel search, which tests the whole code phases in parallel, is impractical in implementation for long PN-code because of its broad search space [2]. Serial search (SS), which detects code phases one-by-one, is inapplicable because many tests are required and the search process is very long [3]. Hybrid search, which tests a block of code phases in parallel, provides a tradeoff of them. Thus, hybrid search becomes the basis of many rapid PN-code acquisition methods. Zero-padding method (ZP) is one of these methods [4]-[6]. By adding $N/2$[1] zeros to extend the incoming samples to length N and with fast Fourier transform (FFT) techniques, ZP can search $N/2+1$[2] code phases in parallel. Scaled acquisition methods have been investigated for rapid PN-code acquisition [8]. By mapping several chips to one chip, the search space is reduced and the search process is speeded up. Since folding is effective to directly reduce the code phases to be searched, extended replica folding acquisition search technique (XFAST) provides another valid approach to accelerate the search process [10], [11]. By folding local signal, the code phases to be searched are directly decreased proportional to local folding number. For instance, conditioned on the local folding number 20, the code phases to be searched are reduced to $1/20$; with local folding number 50, the code phases are decreased to $1/50$. Nevertheless, the degradation, which corresponds to folding, of PN-code correlation properties is proportional to the folding number as well. So the detection performance[3] of XFAST deteriorates. Providing the incoming signal-to-noise ratio (SNR) is high enough that the degradation is insignificant, XFAST is capable of a high search speed. While the incoming SNR cannot meet the condition, its acquisition performance will be discounted and it may even spend more time on acquisition than nonfolding methods such as ZP.

To improve the detection performance, a dual-folding acquisition method (DF) is proposed. DF absorbs the advantage of XFAST, i.e., by folding, the code phases to be searched are directly reduced. To overcome the disadvantage of XFAST in the degradation of PN-code correlation properties, both incoming signal and local signal are folded in DF. With respect to XFAST, the code phases searched in parallel to DF are reduced slightly, but the coherent integration time is greatly extended resulting in the improvement of detection performances. Consequently, the acquisition performance of DF is established in the tradeoff between the benefit of extending coherent integration time and the loss resulting from the degraded PN-code correlation properties. When the incoming SNR is not so high enough that the degradation

Manuscript received October 13, 2007; revised January 14, 2008; accepted March 7, 2008. The associate editor coordinating the review of this paper and approving it for publication was I.-M. Kim.

The authors are with the Department of Electronic Engineering, Tsinghua University, Beijing 100084, China (e-mail: lihong04@mails.tsinghua.edu.cn; {cxw2005, lumq, fzm}@tsinghua.edu.cn).

Digital Object Identifier 10.1109/T-WC.2008.071130

[1]To use FFT effectively, N is often a power of 2.

[2]In some references [4], [5], the code phases searched in parallel are referenced as $N/2$ instead of $N/2+1$.

[3]In this paper, detection performance refers to detection probability and acquisition performance can be evaluated by mean acquisition time.

1536-1276/08$25.00 © 2008 IEEE

of PN-code correlation properties resulting from folding is insignificant for PN-code acquisition, DF has much better acquisition performance than XFAST. Compared with other methods, DF shows its enhancement as well.

The rest of this paper is organized as follows. In Section II, the proposed method is described. In Section III, the performance is analyzed, including the correlation properties of folded PN-code, distribution of observation windows that entirely or partially contain incoming samples, and mean acquisition time. Numerical results are provided in Section IV and conclusions are drawn in Section V.

II. Method Description

Folding is composed of grouping and term-by-term adding [10], [11]. For instance, choose 20480 local code samples and divide them into twenty groups, each containing 1024 elements. Then by term-by-term adding among the twenty groups, 1024 new samples are produced. Subsequently, the search process is conducted on the folded new samples. Thus, by folding the cardinality of cells to be searched is reduced and the search space shrinks.

In contrast to XFAST, which folds only local signal, DF folds both incoming signal and local signal, respectively, as shown in Fig. 1. By folding both incoming signal and local signal, DF extends the coherent integration time, which would mitigate the effect of degraded PN-code correlation properties. Assume that the incoming samples and local code samples are parsed into blocks with length N, and the folding numbers of incoming signal and local signal are K and M, respectively. The code phases searched in parallel are $(M-K)N+1$[4] and the coherent integration time is KN/f_s, where f_s is the sampling frequency. As shown in Fig. 2, with folding numbers $K=2$ and $M=7$, the code phases searched in parallel are $5N+1$ and the coherent integration time is $2N/f_s$. With respect to nonfolding methods that at most search N code phases in parallel, the code phases to be searched for DF are reduced to $1/5$[5]. With the same local folding number, XFAST, which searches $6N+1$ code phases in parallel with coherent integration time N/f_s, the code phases are decreased to $1/6$. Thus, DF has a few more cells to search, but its coherent integration time increases twice. When $M \gg K$, which is often available, the decrease of the code phases searched in parallel is slight but the gain resulting from the extended coherent integration time is noticeable. When detection performance is significant to acquisition performance, the gain can provide great enhancements in shortening the search process.

Similar to other methods, the flaw of extending coherent integration time is its negative effect on frequency. If the coherent integration time is so long that after extending there are much more frequency cells to search, the enhancement of the proposed method will be discounted.

As shown in Fig. 1, the overall algorithm follows.

[4]The code phases searched in parallel are determined by the difference of the folding numbers M and K. In the paper, it is assumed that M is not smaller than K.

[5]Strictly speaking, the search space is less than $1/5$. Since the block length N is often much larger than 1, it is approximately $1/5$. Similar treatments are applied to others.

Step 1. The incoming baseband signal is sampled by analog-to-digital converter at an appropriate rate. Then the samples are processed into complex ones.

Step 2. Choose KN incoming complex samples and fold them into N new samples. Then do FFT on the new samples, followed by complex conjugation and carrier Doppler compensation if needed.

Step 3. Choose MN local code samples and fold them into N new samples, which constitute an observation window, before FFT is done.

Step 4. Multiply the FFT results and perform IFFT.

Step 5. Conduct noncoherent integration processing.

Step 6. If the maximum correlation result (the peak) is larger than a threshold, a temporary detection is declared and is followed by checking [8], [15], [16]. If no peak is larger than the threshold or the checking is a false one, shift $(M-K)N+1$ unfolded local code samples and follow the same process again.

Step 7. After a successful checking, the peak has a code phase resolution of MN samples, which is called ambiguity in Fig. 1. If more accurate code phase is needed, go to the following steps.

Step 8. Take N unfolded local code samples to do FFT; take $N/2$ unfolded incoming samples and pad $N/2$ zeros to extend to length N, followed by FFT and complex conjugation. Multiply the FFT results and perform IFFT.

Step 9. Preserve the first $N/2+1$ elements from the results of Step 8 and discard the others. Conduct noncoherent integration processing.

Step 10. Shift $N/2+1$ unfolded local code samples and follow Step 8 and Step 9 until all the MN samples are tested.

Step 11. The exact incoming code phase can be determined according to the position of the maximum correlation result of Step 10.

In Step 7, the true hypothesis region contains the observation windows that partially cover incoming samples. Step 1 to Step 7 comprises the coarse acquisition of Fig. 1 and Step 8 to Step 11 constitutes the fine acquisition. Indeed, Step 8 to Step 11 comprises the zero-padding method in [4], [5]. In Step 5 and Step 9, if lower false alarm probability is needed, other combing methods would be employed [16]. As for long PN-code acquisition, the time spent on coarse acquisition is much longer than that spent on fine acquisition. Thus, in this paper, the analysis is focused on the coarse acquisition.

III. Performance Analysis

The analysis presented in this section highlights the tradeoff between the total operations performed by the coarse acquisition and the detection performance. We will start with the correlation properties of folded PN-code, which is the basis for analyzing detection performance, and the distribution of observation windows that entirely or partially contain incoming samples, before deriving and analyzing the tradeoff, which is evaluated by mean acquisition time.

A. Notations and Parameters

The following symbols and parameters are adopted in the paper.

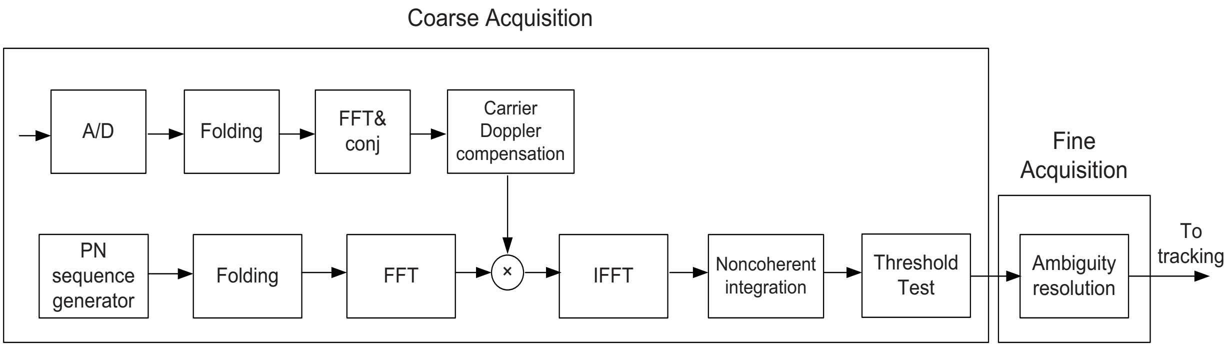

Fig. 1. Proposed dual-folding acquisition method (DF). Before conducting correlation, both incoming signal and local signal are folded, and correlation is conducted on the folded signals. Here, FFT is employed to conduct correlation.

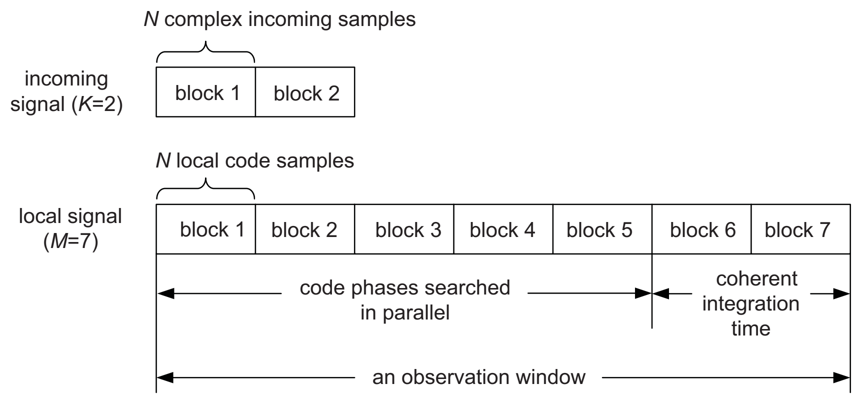

Fig. 2. Concept of folding. Block one and block two of incoming signal are added together term by term to produce a new block, which is called folded incoming signal; block one to block seven of local signal is also added together term by term to produce a new block, which is called folded local signal. Then correlation is conducted on the folded signals. Coherent integration time is determined by the smaller one of K and M. The code phases searched in parallel are proportional to the difference between K and M.

- The signal grouping length (block length) and FFT length: N; folding number of incoming signal (incoming folding number): K; folding number of local signal (local folding number): M.
- Incoming complex samples: s_l $(l = 0, 1, 2, \ldots)$; in-phase components: $s_{I,l} = Ad_{l+\tau}c_{l+\tau}\cos(\omega_D l\Delta t+\varphi)+n_{I,l}$ and quadrature components: $s_{Q,l} = Ad_{l+\tau}c_{l+\tau}\sin(\omega_D l\Delta t + \varphi) + n_{Q,l}$.
- Signal amplitude: A; modulation data: $d_l \in \{-1, +1\}$; PN-code: $c_l \in \{-1, +1\}$. PN-code code is treated as independent identically distributed (i.i.d.) sequence with zero-mean and variance 1.
- Residual carrier frequency: $\omega_D = 2\pi f_D$; unknown code phase of incoming signal: τ; code phase of local signal: δ; unknown incoming carrier phase: φ; sampling interval: Δt; sampling frequency: $f_s = 1/\Delta t$; PN-code chip rate: f_c; the ratio of f_s divided by f_c: w.
- The noises $n_{I,l}$ and $n_{Q,l}$ are assumed to be i.i.d. additive Gaussian white noise (AGWN) with zero-mean and variance σ^2, i.e., $n_{I,l} \sim \Psi(0, \sigma^2)$ and $n_{Q,l} \sim \Psi(0, \sigma^2)$.
- True hypothesis: H_1; false hypothesis: H_0.
- Detection probability for a single cell: $P_d^{(s)}$; detection probability for an observation window: $P_d^{(b)}$; false alarm probability for a single cell: $P_{fa}^{(s)}$; false alarm probability for an observation window: $P_{fa}^{(b)}$.
- The number of code phases to be searched: Θ.
- Inner product: $<>$; the integer part of a: $\lfloor a \rfloor$; the minimum integer not smaller than a: $\lceil a \rceil$.
- The observation window containing the whole incoming samples: D_w; the index of the sample in D_w aligning with the first incoming sample: ϑ; the set of the observation windows entirely or partially containing incoming samples: W.

B. Correlation Properties of Folded PN-code

The complex incoming samples s_l $(l = 0, 1, 2, \ldots)$ are parsed into blocks of size $N \times 1$: $\vec{s}_k = \vec{s}_{I,k} + j\vec{s}_{Q,k}$, where $\vec{s}_{I,k} = [s_{I,kN}, s_{I,kN+1}, \ldots, s_{I,kN+N-1}]^T$ is the in-phase component, $\vec{s}_{Q,k} = [s_{Q,kN}, s_{Q,kN+1}, \ldots, s_{Q,kN+N-1}]^T$ the quadrature component, and k $(k = 0, 1, 2, \ldots, K-1)$ the block index. The folding of the incoming samples yields $\overline{\vec{s}} = \overline{\vec{s}}_I + j\overline{\vec{s}}_Q$, where $\overline{\vec{s}}_I = \mathbf{B}_{s,I}\vec{1}_{K\times 1}$, $\overline{\vec{s}}_Q = \mathbf{B}_{s,Q}\vec{1}_{K\times 1}$, $\mathbf{B}_{s,I} = [\vec{s}_{I,0}, \vec{s}_{I,1}, \ldots, \vec{s}_{I,K-1}]$, $\mathbf{B}_{s,Q} = [\vec{s}_{Q,0}, \vec{s}_{Q,1}, \ldots, \vec{s}_{Q,K-1}]$, and $\vec{1}$ is the summing vector. Local code samples $c_{l+\delta}$ $(l = 0, 1, 2, \ldots)$ are also parsed into blocks of size $N \times 1$: $\vec{r}_m = [c_{mN+\delta}, c_{mN+1+\delta}, \ldots, c_{mN+N-1+\delta}]^T$, where m $(m = 0, 1, 2, \ldots, M-1)$ represents the block index. Then $\vec{r}_m$ are folded into $\overline{\vec{r}} = \mathbf{B}_r\vec{1}_{M\times 1}$, where $\mathbf{B}_r = [\vec{r}_0, \vec{r}_1, \ldots, \vec{r}_{M-1}]$.

Subsequently, the correlation between the folded incoming signal $\overline{\vec{s}}$ and the folded local signal $\overline{\vec{r}}$ produces the in-phase correlation result $C_I =< \overline{\vec{s}}_I, \overline{\vec{r}} >$ and the quadrature correlation result $C_Q =< \overline{\vec{s}}_Q, \overline{\vec{r}} >$. Let us first focus on the in-phase correlation result. Substituting the expressions of $\overline{\vec{s}}_I$ and $\overline{\vec{r}}$ into C_I, it follows

$$\begin{aligned} C_I &= \sum_{m=0}^{M-1}\sum_{k=0}^{K-1}\sum_{l=0}^{N-1} s_{I,kN+l}c_{mN+l+\delta} \\ &= \sum_{m=0}^{M-1}\sum_{k=0}^{K-1}\sum_{l=0}^{N-1} Ad_{kN+l+\tau}c_{kN+l+\tau}c_{mN+l+\delta} \\ &\quad \times \cos\left(\omega_D(kN+l)\Delta t+\varphi\right) \\ &\quad + \sum_{m=0}^{M-1}\sum_{k=0}^{K-1}\sum_{l=0}^{N-1} n_{I,kN+l}c_{mN+l+\delta} \end{aligned} \tag{1}$$

The in-phase correlation result C_I is composed of three items: coherent integration, self-noise, and AGWN. Provided there are $n(n = 0, 1, 2, \ldots, KN)$ unfolded incoming samples of $\overline{\vec{s}}_I$, which derives from KN incoming samples, falling into the folded local signal $\overline{\vec{r}}$, $s_{I,g}$ aligns with $c_{h+\delta}$ and $s_{I,g+n-1}$ with $c_{h+\delta+n-1}$, then the coherent integration item Ω_I of in-phase correlation result can be written as

$$\Omega_I = \sum_{l=0}^{n-1} Ad_\tau c_{l+g+\tau}c_{l+h+\delta}\cos(\omega_D l\Delta t+\varphi_1) \tag{2}$$

where $\varphi_1 = g\omega_D\Delta t + \varphi$. g is the index of the first incoming sample aligning with local code sample and h is the index of the first local code sample aligning with incoming sample. The modulation data is assumed to be a constant d_τ within the coherent integration time[6]. Note that $n = 0$ implies that there is no coherent integration item and $n = KN$ means that local signal covers all the incoming samples. The mean value of Ω_I is

$$E_{\Omega_I} = Ad_\tau R_i(p)\sum_{l=0}^{n-1}\cos(\omega_D l\Delta t+\varphi_1),\ i=0,1 \tag{3}$$

where the residual code phase offset p is equal to $\big((g+\tau)-(h+\delta)\big) - \lfloor (g+\tau)-(h+\delta)\rfloor$ and $R_i(p) = \begin{cases}1-|p|, & H_1\\ 0, & H_0\end{cases}$. [17]. Since the variance of $\sum_{l=0}^{n-1} Ad_\tau c_{l+g+\tau}c_{l+h+\delta}$ is not larger than $wnG_i(p)A^2$, where $G_i(p) = \begin{cases}p^2, & H_1\\ (1-|p|)^2, & H_0\end{cases}$. [17], as a pessimistic approximation, the variance of Ω_I is $wnG_i(p)A^2$. For a large class of codes, with central limit theorem, the coherent integration item closely resembles a Gaussian random variable, so $\Omega_I \sim \Psi\big(E_{\Omega_I}, wnG_i(p)A^2\big)$.

The noise $n_{I,l}$ is treated as i.i.d. AGWN with zero-mean and variance σ^2, so the summation of all the multiplication between Gaussian noise and PN-code, i.e., the AGWN item, follows

$$\sum_{m=0}^{M-1}\sum_{k=0}^{K-1}\sum_{l=0}^{N-1} n_{I,kN+l}\, c_{mN+l+\sigma} \sim \Psi\left(0, KMN\sigma^2\right) \tag{4}$$

The rest of in-phase correlation result constitutes the self-noise item. With central limit theorem, it closely resembles a Gaussian random variable. Conditioned on $p = 0$, which is a pessimistic approximation [17], the self-noise item follows $\Psi\left(0, w\left(KMN-n\right)A^2\right)$.

Therefore, the summation of coherent integration item, self-noise item, and AGWN item, i.e., the in-phase correlation result C_I, follows

$$\begin{aligned} &C_I \sim \\ &\quad \Psi\big(E_{\Omega_I}, KMN(\sigma^2+wA^2)+wnG_i(p)A^2-wnA^2\big), \\ &\qquad\qquad\qquad\qquad\qquad i=0,1 \end{aligned} \tag{5}$$

Similarly, the quadrature correlation result C_Q follows

$$\begin{aligned} &C_Q \sim \\ &\quad \Psi\big(E_{\Omega_Q}, KMN(\sigma^2+wA^2)+wnG_i(p)A^2-wnA^2\big), \\ &\qquad\qquad\qquad\qquad\qquad i=0,1 \end{aligned} \tag{6}$$

where $E_{\Omega_Q} = Ad_\tau R_i\left(p\right)\sum_{l=0}^{n-1}\sin\left(\omega_D l\Delta t+\varphi_1\right)$ represents the mean value of the coherent integration item of quadrature correlation result.

After power detection, the envelope $\xi = \sqrt{C_I^2 + C_Q^2}$ is produced. Conditioned on n, p, and H_i, for a single cell ξ follows Rice distribution [18] and the probability density function is

$$\begin{aligned} f_\xi\left(x\left|n,p,H_i\right.\right) = \frac{x}{\sigma_{H_i}^2}\exp\left\{-\frac{x^2+\mu_i^2}{2\sigma_{H_i}^2}\right\} I_0\left(\frac{x\mu_i}{\sigma_{H_i}^2}\right), \\ x\geq 0,\ i=0,1 \end{aligned} \tag{7}$$

where the variance is $\sigma_{H_i}^2 = KMN\left(\sigma^2+wA^2\right) + wnG_i\left(p\right)A^2 - wnA^2$. $I_0()$ is the zeroth-order modified Bessel function of the first kind and can be written as $I_0\left(\lambda\right) = \sum_{l=0}^{\infty}\frac{(\lambda/2)^{2l}}{l!\Gamma(l+1)}$ for computation [18]. Another item is

$$\begin{aligned} \mu_i^2 &= E_{\Omega_I}^2 + E_{\Omega_Q}^2 \\ &\approx n^2A^2R_i^2\left(p\right)\rho^2 \end{aligned} \tag{8}$$

where $\rho^2 = \mathrm{sinc}^2\left(\pi f_D n\Delta t\right)$ represents the loss resulting from the residual carrier frequency f_D. The advantage of extending coherent integration time of DF is reflected by n^2 of Eq. 8, and the drawback by ρ^2.

In power detection, according to the false alarm probability for a single cell $P_{fa}^{(s)} = \int_{V_t}^{+\infty} f_\xi\left(x\left|0,p\,,H_0\right.\right)dx$, we can derive the threshold $V_t = \sqrt{-2KMN\left(\sigma^2+wA^2\right)\ln P_{fa}^{(s)}}$ and the detection probability for a single cell

$$P_{d,n,p}^{(s)} = Q_1\left(\frac{\mu_1}{\sigma_{H_1}}, \frac{V_t}{\sigma_{H_1}}\right) \tag{9}$$

where Q_1 is Marcum's Q function and

$$\sigma_{H_1}^2 = KMN\left(\sigma^2+wA^2\right) + wnp^2A^2 - wnA^2. \tag{10}$$

C. Distribution of Observation Windows

Conditioned on folding numbers K, M and block length N, within an observation window, the proposed method searches $(M-K)N+1$ code phases in parallel, and tests N envelops of ξ. If the maximum correlation result $\xi_{\max}^{(b)} = \max_{0\leq i\leq N-1}\{\xi_i\}$ of an observation window is larger than a threshold, a temporary detection is declared and is followed by checking. Otherwise,

[6]The assumption is valid when (a) coherent integration time is much shorter than the duration of modulation data, (b) pilot channel where there is no modulation data is used. The effect of modulation data on acquisition can refer to [2].

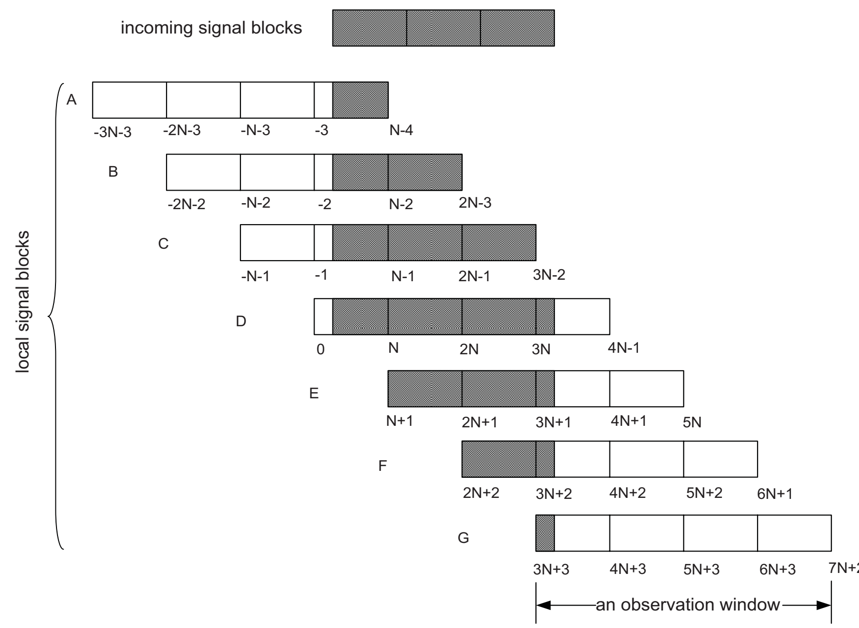

Fig. 3. Observation windows that entirely or partially contain incoming samples. Only one observation window D entirely contains the incoming samples but multiple observation windows A, B, C, E, F, and G partially contain them. Observation windows A, B, and C constitute subset I, observation window D constitutes subset II, observation windows E, F, and G constitute subset III, and the three subsets constitute set W. The farthest observation window from observation window D is observation window A in subset I, and observation window G in subset III. Here local folding number is 4, incoming folding number is 3, and block length is N. Note that before conducting correlation both incoming signal blocks and local signal blocks would be added together, respectively, to form folded incoming signal $\vec{s}$ and folded local signal $\vec{r}$.

TABLE I
FORMULAE TO COMPUTE $n_{i|\vartheta}$, CONDITIONED ON M, K, AND N.

Subset	Parameters		Expression of $n_{i\|\vartheta}$	Range of index	Range of ϑ
I	$a_1 = 0$	$b_1 = 0$	none	none	none
		$b_1 \geq 0$	$n_{i\|\vartheta} = KN - \vartheta - 1$	$i = 1$	$\vartheta = 0, 1, 2, \ldots, b_1 - 1$
	$a_1 \geq 1$	$b_1 = 0$	$n_{i\|\vartheta} = KN - (i-1)((M-K)N+1) - \vartheta - 1$	$i = 1, 2, \ldots, a_1$	$\vartheta = 0, 1, 2, \ldots, (M-K)N$
		$b_1 \geq 1$	$n_{i\|\vartheta} = KN - (i-1)((M-K)N+1) - \vartheta - 1$	$i = 1, 2, \ldots, a_1$	$\vartheta = 0, 1, 2, \ldots, (M-K)N$
			$n_{i\|\vartheta} = KN - (i-1)((M-K)N+1) - \vartheta - 1$	$i = a_1 + 1$	$\vartheta = 0, 1, 2, \ldots, b_1 - 1$
II	none		$n = KN$	$i = 1$	$\vartheta = 0, 1, 2, \ldots, (M-K)N$
III	$a_2 = 0$		none	none	none
	$a_2 = 1$	$b_2 = 0$	none	none	none
		$b_2 \geq 1$	$n_{i\|\vartheta} = 2KN - MN + \vartheta - 1$	$i = 1$	$\vartheta = a_3, a_3 + 1, \ldots, (M-K)N$
	$a_2 \geq 2$	$b_2 = 0$	$n_{i\|\vartheta} = KN - i((M-K)N+1) + \vartheta$	$i = 1, 2, \ldots, a_2 - 1$	$\vartheta = 0, 1, 2, \ldots, (M-K)N$
		$b_2 \geq 1$	$n_{i\|\vartheta} = KN - i((M-K)N+1) + \vartheta$	$i = 1, 2, \ldots, a_2 - 1$	$\vartheta = 0, 1, 2, \ldots, (M-K)N$
			$n_{i\|\vartheta} = KN - i((M-K)N+1) + \vartheta$	$i = a_2$	$\vartheta = a_3, a_3 + 1, \ldots, (M-K)N$

(1) When there is no observation window that contains incoming samples, the corresponding items are recorded as none. Generally, the block length is much larger than one; hence, when a_2 is equal to one, b_2 is larger than zero.
(2) In subset II, the observation window D_w always contains KN incoming samples and its corresponding parameter item is recorded as none.

shift $(M-K)N+1$ local code samples and detect another observation window until a larger peak is found, followed by a successful checking.

With the above searching strategy, provided that the incoming samples fall into the search space, there is only one observation window that entirely contains the incoming samples but there are multiple ones that partially contain them, as shown in Fig. 3. Denote the observation window that contains the whole incoming samples as D_w and define the index of the first sample in D_w as zero. Denote the index of the sample in D_w aligning with the first incoming sample as ϑ. To cover the entire incoming samples, ϑ is between zero and $(M-K)N$. Otherwise, the observation window D_w cannot contain the entire incoming samples.

Referenced to the observation window D_w, the set W composed of the observation windows that entirely or partially contain the incoming samples can be divided into three subsets. The first subset consists of the observation windows that partially contain the incoming samples before the entire incoming samples fall into the observation window D_w. The second subset contains only one observation window, i.e., D_w. The rest of the observation windows in set W constitute the third subset. As shown in Fig. 3, the first subset refers to observation windows A, B and C, the second subset implies observation window D, and the third subset comprises observation windows E, F, and G.

Referring to subset I, the observation windows at most cover $KN-1$ incoming samples. The difference of code phases between adjacent observation windows is $(M-K)N+1$.

Thus, we can define

$$KN-1 = a_1\left(\left(M-K\right)N+1\right)+b_1 \quad (11)$$

where the coefficients a_1 and b_1 are non-negative integers, and b_1 is between zero and $(M-K)N$. The quotient a_1 indicates the number of observation windows partially covering $KN-1$ incoming samples when ϑ is between zero and $(M-K)N$. The reminder b_1 represents the code phase of the incoming sample that corresponds to the farthest observation window of subset I from the observation window D_w withdraws from subset I. Therefore, within subset I, when $b_1 = 0$ there are a_1 observation windows. Otherwise, there are a_1+1 observation windows when $\vartheta \in [0, b_1-1]$ and a_1 observation windows when $\vartheta \in [b_1, (M-K)N]$.

Once an observation window has no intersection with observation window D_w, it must not cover any incoming sample because the entire incoming samples are assumed to fall into the observation window D_w. There are MN samples in observation window D_w and the difference of code phases between adjacent observation windows is $(M-K)N+1$. Hence, for subset III we can determine the number of observation windows intersecting with D_w by

$$MN = a_2\left(\left(M-K\right)N+1\right)+b_2 \quad (12)$$

where the coefficients a_2 and b_2 are non-negative integers and b_2 is between zero and $(M-K)N$. When b_2 is zero, Eq. 12 means that the index of the first sample of the farthest observation window of subset III from observation window D_w is MN, which is larger than $MN-1$ the largest index of observation window D_w. Hence, the farthest observation window has no intersection with observation window D_w. When b_2 is larger than zero, the index of the first sample of the farthest observation window from observation window D_w is not larger than $MN-1$. Hence, the farthest observation window has at least one common sample with observation window D_w. Therefore, when b_2 is zero there are a_2-1 observation windows in subset III. Otherwise, there are a_2 observation windows and the index of the incoming sample that corresponds to the farthest observation window from observation window D_w entering subset III is a_3, which is derived from

$$a_3 = (M-K)N - b_2 + 1 \quad (13)$$

Conditioned on folding numbers M, K and block length N, the formulae of $n_{i|\vartheta}$, which represents the number of incoming samples falling into the i-th observation window of the corresponding subset, are illustrated in Table. I.

D. Mean Acquisition Time

Conditioned on the folding numbers M, K, block length N, and the index ϑ, the number of observation windows within set W is denoted as $C_{|\vartheta}$, which is the combination of the observation windows in subset I, subset II, and subset III. In set W, each observation window comprises a H_1 region with at least $2\lfloor f_s/f_c \rfloor - 1$ cells[7]. Conditioned on the residual code phase offset of the $\lfloor f_s/f_c \rfloor$-th cell is θ , where $\theta \in (-f_c/f_s, f_c/f_s)$, the residual code phase offsets of these cells can be represented by

$$p_{j|\theta} = (\lfloor f_s/f_c \rfloor - j)f_c/f_s + \theta, \qquad j = 1, 2, \ldots, 2\lfloor f_s/f_c \rfloor - 1 \quad (14)$$

In an observation window of set W, if the maximum correlation result $\xi^{(b)}_{\max} = \max_{0 \le i \le N-1}\{\xi_i\}$ is larger than a threshold, a temporary detection is declared and is followed by checking. If the checking is true, the observation window instead of only the maximum correlation result will be tested, which constitutes fine acquisition. Therefore, in coarse acquisition, the detection probability for the i-th observation window of set W is the probability that one of the correlation results is larger than threshold. Conditioned on ϑ and θ, the detection probability is

$$P^{(b)}_{d,i|\vartheta,\theta} = 1 - (1 - P^{(s)}_{fa})^{(N-2\lfloor f_s/f_c \rfloor+1)} \prod_{j=1}^{2\lfloor f_s/f_c \rfloor - 1} (1 - P^{(s)}_{d,n_{i|\vartheta},p_{j|\theta}}), \qquad i = 1, 2, 3, \ldots, C_{|\vartheta} \quad (15)$$

where $P^{(s)}_{d,n_{i|\vartheta},p_{j|\theta}}$ is the detection probability for a single cell with $n_{i|\vartheta}\Delta t$ coherent integration time and residual code phase offset $p_{j|\theta}$. Note the choice of $n_{i|\vartheta}$, where i is the index of the observation windows in set W.

The false alarm probability for other observation windows that contain no incoming sample is

$$P^{(b)}_{fa} = 1 - (1 - P^{(s)}_{fa})^N. \quad (16)$$

Providing there are Θ code phases to search, with the proposed method DF, in each observation window $(M-K)N+1$ code phases are searched in parallel. Therefore, there are

$$\Lambda = \left\lceil \frac{\Theta}{(M-K)N+1} \right\rceil \quad (17)$$

observation windows to test per single run. Denote T_D as the delay in detecting an observation window and κT_D as the punishment for a false alarm. Then the search process can be described by a flow-graph diagram [3], a portion of which is shown in Fig. 4. Here, FA represents the false-alarm state and ACQ the absorbing (correct-acquisition) state. $\{\pi_i\}$ ($i = 1, 2, ..., \Lambda$ and $\sum_{i=1}^{\Lambda} \pi_i = 1$), which is often assumed to be a uniform one, is the priori distribution of starting the search process from which observation window. "$\Lambda + 1$" represents the $C_{|\vartheta}$ observation windows within set W.

Let $H_{DET,i|\vartheta,\theta}(z)$ and $H_{M,i|\vartheta,\theta}(z)$ $(i = 1, 2, ..., C_{|\vartheta})$ denote the individual detection and miss gains of each observation window within node "$\Lambda + 1$". Then the detection

[7]Practically, the block length N is often much larger than one such as 1024, 2048, etc.; hence, the probability of $n_{i|\vartheta}$ larger than $2\lfloor f_s/f_c \rfloor - 1$ is nearly 1. Thus, the probability of the number of cells in H_1 larger than $2\lfloor f_s/f_c \rfloor - 1$ is closely 1.

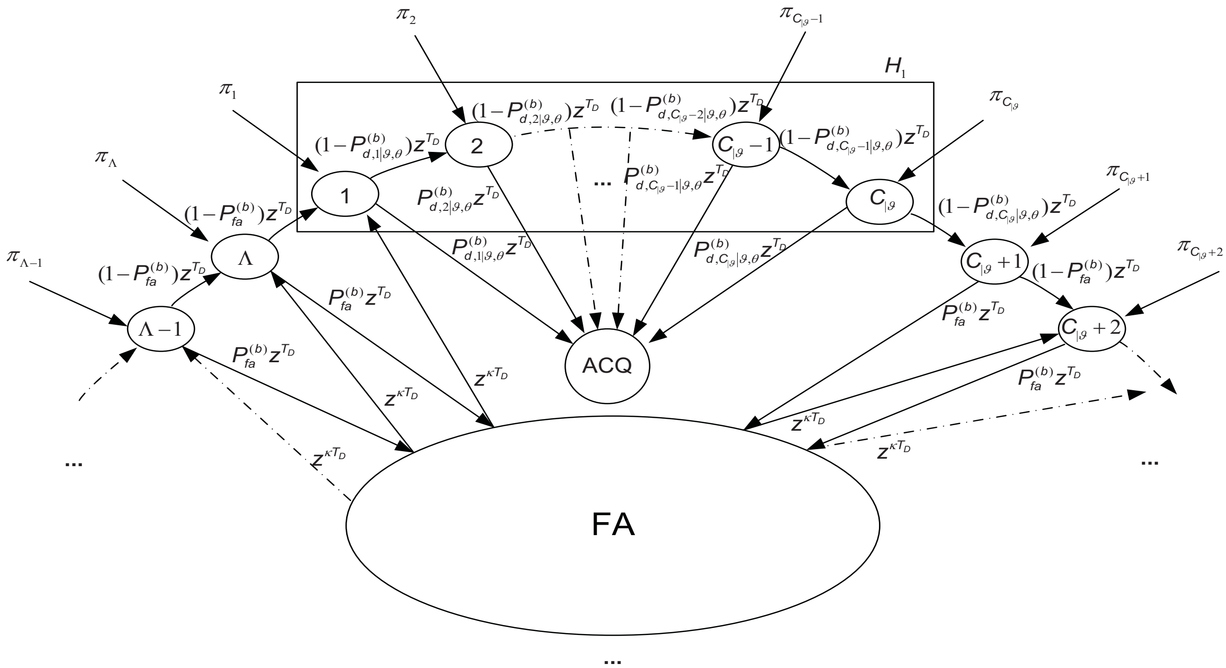

Fig. 4. A portion of the flow-graph diagram for the proposed method.

gain from node "$\Lambda+1$" to node ACQ is

$$\begin{aligned} H_{DET|\vartheta,\theta}(z) &= H_{DET,1|\vartheta,\theta}(z) \\ &\quad + \sum_{j=2}^{C_{|\vartheta}} \prod_{i=1}^{j-1} H_{M,i|\vartheta,\theta}(z) H_{DET,j|\vartheta,\theta}(z) \\ &= P^{(b)}_{d,1|\vartheta,\theta} z^{T_D} \\ &\quad + \sum_{j=2}^{C_{|\vartheta}} \prod_{i=1}^{j-1} (1-P^{(b)}_{d,i|\vartheta,\theta}) P^{(b)}_{d,j|\vartheta,\theta} z^{jT_D} \end{aligned} \tag{18}$$

And, the miss gain leading node "$\Lambda+1$" to node $C_{|\vartheta}+1$ follows

$$\begin{aligned} H_{M|\vartheta,\theta}(z) &= \prod_{i=1}^{C_{|\vartheta}} H_{M,i|\vartheta,\theta}(z) \\ &= \prod_{i=1}^{C_{|\vartheta}} (1-P^{(b)}_{d,i|\vartheta,\theta}) z^{C_{|\vartheta} T_D} \end{aligned} \tag{19}$$

The gain $H_0(z)$ connecting two successive nodes $(i, i+1)$ $(i = C_{|\vartheta}+1, C_{|\vartheta}+2, ..., \Lambda\ )$ is

$$H_0(z) = (1-P^{(b)}_{fa}) z^{T_D} + P^{(b)}_{fa} z^{(\kappa+1)T_D} \tag{20}$$

Provided that the priori distribution $\{\pi_i\}$ is a uniform one, the generating function is [3]

$$\begin{aligned} &\mathrm{P}_{ACQ|\vartheta,\theta}(z) = \\ &\quad \frac{H_{DET|\vartheta,\theta}(z)}{\Lambda\left(1 - H_{M|\vartheta,\theta}(z) H_0^{\Lambda-C_{|\vartheta}}(z)\right)} \\ &\quad \left\{ \frac{H_0(z)\left(1-H_0^{\Lambda-C_{|\vartheta}}(z)\right)}{1-H_0(z)} + C_{|\vartheta} \right\} \end{aligned} \tag{21}$$

Then, the conditional mean acquisition time follows

$$\begin{aligned} E\left(T_{ACQ|\vartheta,\theta}\right) &= \left.\frac{d\mathrm{P}_{ACQ|\vartheta,\theta}(z)}{dz}\right|_{z=1} \\ &= \frac{T_D}{P^{(b)}_{d,1|\vartheta,\theta} + \sum\limits_{j=2}^{C_{|\vartheta}} \prod\limits_{i=1}^{j-1} (1-P^{(b)}_{d,i|\vartheta,\theta}) P^{(b)}_{d,j|\vartheta,\theta}} \\ &\quad \times \Bigg\{ P^{(b)}_{d,1|\vartheta,\theta} + \sum_{j=2}^{C_{|\vartheta}} \prod_{i=1}^{j-1} (1-P^{(b)}_{d,i|\vartheta,\theta}) P^{(b)}_{d,j|\vartheta,\theta}\, j \\ &\quad + C_{|\vartheta} \prod_{i=1}^{C_{|\vartheta}} (1-P^{(b)}_{d,i|\vartheta,\theta}) + \left(\Lambda - C_{|\vartheta}\right)\left(1+\kappa P^{(b)}_{fa}\right) \\ &\quad - \left(\Lambda - C_{|\vartheta}\right)\left(1+\kappa P^{(b)}_{fa}\right) \frac{\Lambda + C_{|\vartheta} - 1}{2\Lambda} \\ &\quad \times \left(P^{(b)}_{d,1|\vartheta,\theta} + \sum_{j=2}^{C_{|\vartheta}} \prod_{i=1}^{j-1} (1-P^{(b)}_{d,i|\vartheta,\theta}) P^{(b)}_{d,j|\vartheta,\theta} \right) \Bigg\} \end{aligned} \tag{22}$$

and the mean acquisition time is

$$\begin{aligned} &E\left(T_{ACQ}\right) = \\ &\quad \sum_{l=0}^{(M-K)N} \lambda_l \int_{-f_c/f_s}^{f_c/f_s} f(\theta) E\left(T_{ACQ|\vartheta=l,\theta}\right) d\theta \end{aligned} \tag{23}$$

where $\left\{\lambda_l \left| \sum_{l=0}^{(M-K)N} \lambda_l = 1 \right.\right\}$ represents the distribution of ϑ, and $f(\theta)$ is the probability density function of θ. Provided that the distribution of ϑ is a uniform one and θ is zero, then the mean acquisition time reduces to

$$\begin{aligned} &E\left(T_{ACQ}\right) = \\ &\quad \frac{1}{(M-K)N+1} \sum_{l=0}^{(M-K)N} E\left(T_{ACQ|\vartheta=l,0}\right). \end{aligned} \tag{24}$$

IV. Results and Discussions

In this section, we present the numerical results of coarse acquisition for the detection probability, mean acquisition time, and performance comparisons during SS, ZP, XFAST, and DF, as a function of SNR for a fixed false alarm probability.

GPS P-code, which is a typical long PN-code with chip rate 10.23 Mchip/s and a period of seven days [19], is employed to check detection performance. For simplicity of computation, sampling frequency f_s is set as 10.23 MHz and residual code phase offset θ is set as zero; both $\{\pi_i\}$ and ϑ are assumed to follow uniform distribution; the false alarm probability for a single cell is set as 10^{-5} for SS, ZP, XFAST, and DF; the number of code phases to be searched is set as $\Theta = 10^7$; noncoherent integration number is set as one. Referring to XFAST and DF, the operations of false alarm are proportional to the ambiguity resulting from folding; hence, the false alarm punishment is set as $\kappa = M$ for XFAST and DF. As for SS and ZP, since there is no the ambiguity resulting from folding, their false alarm punishment is set as $\kappa = 1$.

Under these assumptions, the mean acquisition time of SS is [3]

$$E\left(T_{ACQ}^{(SS)}\right) = \frac{T_D}{P_d^{(s,SS)}}\left\{1+\left(1+\kappa P_{fa}^{(s,SS)}\right)\frac{\Theta-1}{2}\left(2-P_d^{(s,SS)}\right)\right\} \quad (25)$$

where $P_{fa}^{(s,SS)}$ is the false alarm probability for a single cell and $P_d^{(s,SS)}$ the detection probability. ZP is capable of searching $N/2+1$ code phases in parallel with FFT techniques of length N. Since after IFFT only the first $N/2+1$ correlation results are valid, there is no observation window partially containing the $N/2$ incoming samples. Therefore, the mean acquisition time of ZP follows

$$E\left(T_{ACQ}^{(ZP)}\right) = \frac{T_D}{P_d^{(b,ZP)}}\left\{1+\left(1+\kappa P_{fa}^{(b,ZP)}\right)\frac{\Lambda^{(ZP)}-1}{2}\left(2-P_d^{(b,ZP)}\right)\right\} \quad (26)$$

where $\Lambda^{(ZP)} = \left\lceil \frac{\Theta}{N/2+1} \right\rceil$ is the number of observation windows, $P_{fa}^{(b,ZP)} = 1-\left(1-P_{fa}^{(s,ZP)}\right)^{N/2+1}$ the block false alarm probability, and $P_d^{(b,ZP)}$ the block detection probability which can be derived from Eq. 15. $P_{fa}^{(s,ZP)}$ is the false alarm probability for a single cell of ZP and can be obtained with similar analysis of DF. The mean acquisition time of XFAST can be obtained from the formulae of DF with $K = 1$.

A. Detection Performance

Fig. 5 reports the benefits and losses of DF with respect to other methods in detection performance. After folding the PN-code correlation properties are degraded and the degradation is reflected by the detection probability for a single cell. With respect to the nonfolding method SS, the folding methods XFAST and DF have worse detection performance. To improve the detection performance, the proposed method DF enlarges coherent integration time by folding both incoming signal and local signal. Fig. 5(a) demonstrates that, compared with XFAST, with the same local folding number, DF improves the detection performance. The gain is about 3 dB when incoming folding number is two, and 6 dB when incoming folding number is four. Fig. 5(b) illustrates that, with the same capability of searching code phases in parallel, DF outperforms XFAST in detection performance as well.

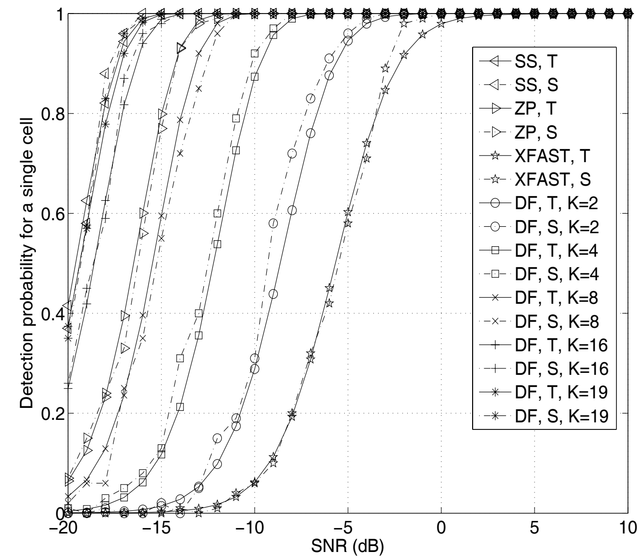

(a)

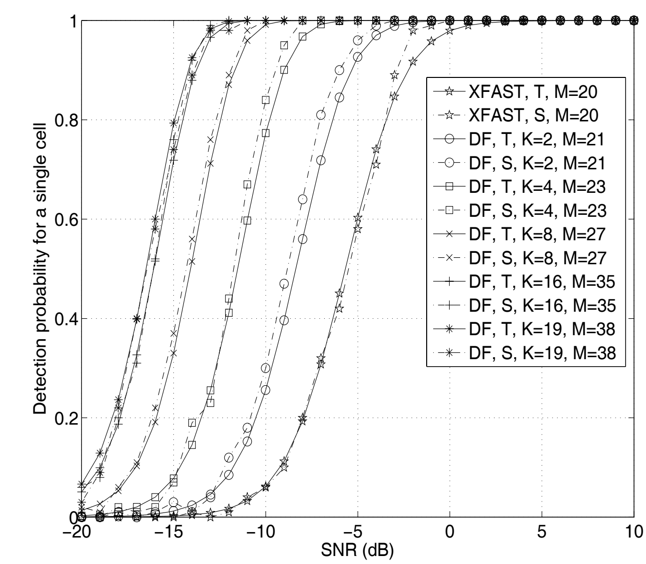

(b)

Fig. 5. Theoretical (continuous line, 'T') and simulation (dashed line, 'S') results for detection probability for a single cell. Block length is 1024 and residual carrier frequency is zero. (a) XFAST and DF have the same local folding number 20. (b) XFAST and DF have the same capability of searching code phases in parallel.

ZP is another nonfolding method with coherent integration time $N\Delta t/2$ less than $N\Delta t$ of SS. Hence, ZP has worse detection performance than SS. The detection performance is relevant to PN-code correlation properties and coherent integration time. ZP has better PN-code correlation properties but

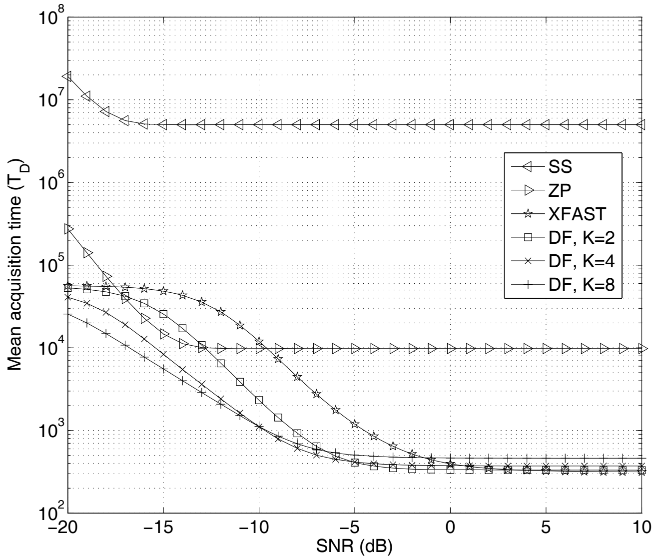

(a)

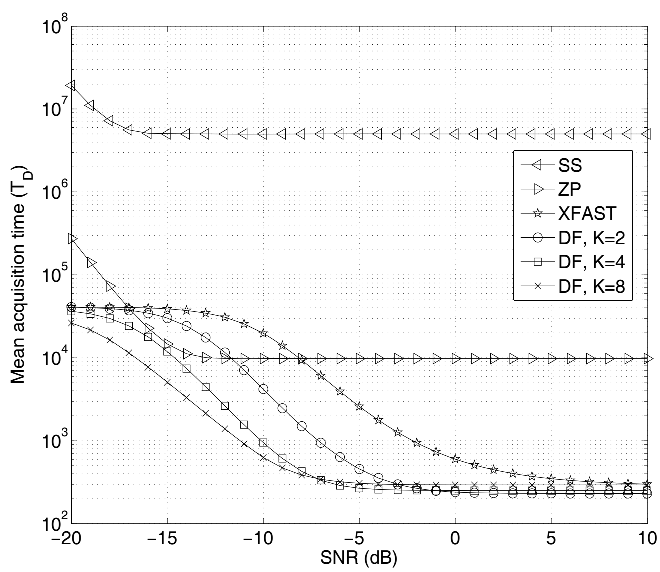

(b)

Fig. 6. Mean acquisition time as a function of SNR. Block length is 1024, residual carrier frequency 300 Hz and local folding number (a) 20 (b) 30.

shorter coherent integration time than XFAST and DF. Consequently, ZP has better detection performance than XFAST and DF with small incoming folding number. However, when the incoming folding number is increased, DF has longer coherent integration time and consequently better detection performance than ZP, as shown in Fig. 5(a) when $K = 16$ and 19.

B. Acquisition Performance

Fig. 6(a) shows the acquisition performance of four methods in mean acquisition time. Compared with SS, three hybrid search methods ZP, XFAST and DF have short mean acquisition time. By folding local signal, XFAST decreases the cardinality of code phases; hence, when the incoming SNR is not less than -9 dB, XFAST consumes less acquisition time than ZP. However, folding degrades the PN-code correlation properties and the degradation is reflected by the acquisition time as well. Fig. 6(a) shows that when the incoming SNR is between -17 dB and -10 dB, XFAST has longer acquisition time than ZP. By folding both incoming signal and local signal to extend coherent integration time, the proposed method DF diminishes the degradation of folded PN-code correlation properties and the enhancement is plotted in Fig. 6(a). When the incoming SNR is not larger than -2 dB, DF with incoming folding number eight spends the least acquisition time than ZP and XFAST. With respect to XFSAT, the gain of DF comes from the extended coherent integration time at the expense of decrease in searching code phases in parallel. When the incoming SNR is high, the importance of extending coherent integration time decreases and the expense appears. As shown in Fig. 6(a), when incoming SNR is not less than -1 dB, DF with incoming folding number eight has longer mean acquisition time than XFAST.

Fig. 6(a) illustrates the mean acquisition time of XFAST and DF seems to be saturated when the incoming signal is weak. Because when the incoming SNR is low the improvement of detection probability that corresponds to the increase of incoming SNR is minor. For instance, the detection probability for a single cell of XFAST is 0.0002 corresponding to the incoming SNR -20 dB, 0.0003 to the incoming SNR -19 dB, 0.0005 to the incoming SNR -18 dB, and 0.0008 to the incoming SNR -17 dB.

Fig. 6(b) reports the effect of local folding number on the proposed method. With larger local folding number, the code phases searched in parallel are increased and the positive effect is represented in the decrease of mean acquisition time. As shown in Fig. 6(a) and (b), with the same incoming folding number 2, DF with local folding number 30 consumes less acquisition time than DF with local folding number 20 when the incoming SNR is larger than -4 dB. On the other hand, the increase in local folding number has a negative effect on PN-code correlation properties, which acts as a deterioration for detection performance and increases mean acquisition time. Compared with Fig. 6(a), Fig. 6(b) shows that, with the same incoming folding number 8, DF with local folding number 30 consumes more acquisition time than DF with local folding number 20 when incoming SNR is not larger than -15 dB.

Fig. 7 focuses on the effect of block length on acquisition performance. Compared with Fig. 6(a), Fig. 7 shows that when the block length is increased the range of DF outperforming XFAST decreases. One factor is that after the block length is extended XFAST has longer coherent integration time, which would improve the detection performance and decrease the mean acquisition time. With respect to XFAST, the gain of DF is derived from the extended coherent integration time. So when the coherent integration time of XFAST is enlarged, the importance of the gain decreases. The other factor is that the larger the block length the more notable is the negative effect of extending coherent integration time on frequency. For instance, with the same folding numbers $K = 8$ and $M = 20$, the loss due to the negative effect which can be evaluated by $\mathrm{sinc}^2(\pi f_D K N \Delta t)$ (Eq. 8), is 0.84 dB for block length 1024 but 3.6 dB for block length 2048.

Fig. 7 shows that the enhancement of DF with incoming

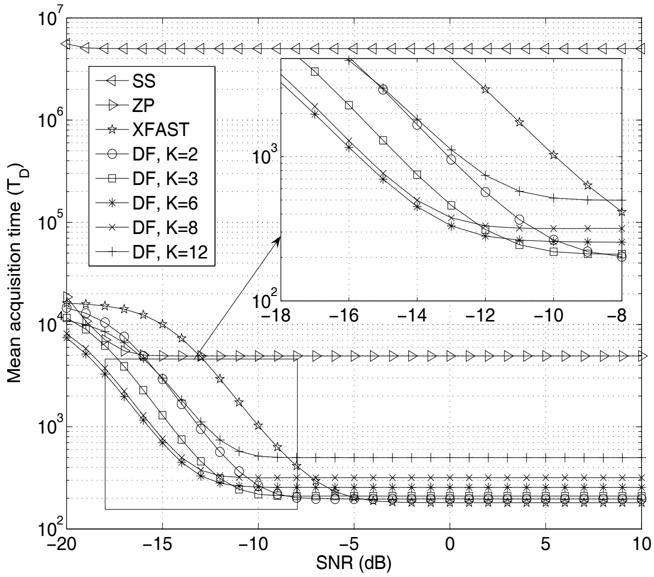

Fig. 7. Effect of block length on acquisition performance. Block length is 2048, residual carrier frequency 300 Hz, and local folding number 20.

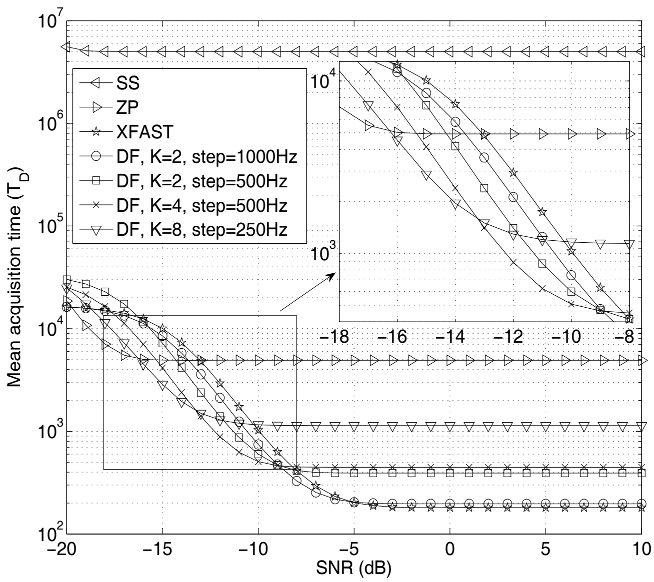

Fig. 8. Effect of residual carrier frequency on acquisition performance. The block length is 2048, residual carrier frequency 1000 Hz, and local folding number 20 for both XFAST and DF. Step represents the frequency bin size.

folding numbers 8 and 12 is negative with respect to DF with incoming folding number 6, which illustrates a principle to design the incoming folding number. The larger the incoming folding number, the longer is the coherent integration time but the fewer are the code phases searched in parallel. So the gain of extending coherent integration time must be incremental. From Eq. 8 and Eq. 10, by comparing the detection performance between DF and XFAST, which is the special case of DF with incoming folding number 1, the principle can be represented by

$$\frac{d}{dK}\left(K\mathrm{sinc}^2\left(\pi f_D K N \Delta t\right)\right) > 0 \tag{27}$$

Finally, we consider the negative effect of extending coherent integration time on frequency. The longer the coherent integration time, the more evident is the negative effect. To diminish the negative effect, one way is to divide the frequency bin size into smaller ones. As shown in Fig. 8, although after dividing the frequency bin size into smaller ones the cells to be searched are increased greatly, with the same incoming folding number 2, DF with frequency step 500 Hz consumes less acquisition time than DF with frequency step 1000 Hz when the incoming SNR is between -15 dB and -9 dB. Nevertheless, when the incoming SNR is high, the improvement from dividing frequency bin size into smaller ones is trivial. Furthermore, due to the increase in cells resulting from finer frequency bin size, the mean acquisition time will increase and Fig. 8 demonstrates this case. With the same incoming folding number 2, DF with frequency step 500 Hz spends more time on acquisition than DF with frequency step 1000 Hz when the incoming SNR is not less than -8 dB.

V. Conclusion

This paper has presented a dual-folding method for long PN-code acquisition. Compared with nonfolding methods SS and ZP, the proposed method DF takes the advantage of reducing the code phases to be searched by folding local signal to shorten mean acquisition time. With respect to XFAST, the first folding method in long PN-code acquisition, DF extends coherent integration time by folding both incoming signal and local signal, to improve detection performance. By considering this advantage, DF broadens the range of XFAST where folding methods outperform nonfolding methods, especially when detection performance is more important than the capability of searching code phases in parallel. The enhancement of DF with respect to SS, ZP, and XFAST has been demonstrated by numerical results and it is relevant to the factors, such as block length, incoming folding number, local folding number, and residual carrier frequency.

References

[1] R. Pickholtz., D. Schilliing, and L. Milstein, "Theory of spread-spectrum communications–a tutorial," *IEEE Trans. Commun.*, vol. 30, pp. 855-884, May 1982.

[2] U. Cheng, W. J. Hurd, and J. I. Statman, "Spread spectrum code acquisition in the presence of Doppler shift and data modulation," *IEEE Trans. Commun.*, vol. 38, no. 2, pp.241-250, Feb. 1990.

[3] A. Polydoros and G. L. Weber, "A unified approach to serial search spread-spectrum code acquisition-part I & II," *IEEE Trans. Commun.*, vol. 32, no. 5, pp. 542-560, May 1984.

[4] J. B. Y. Tsui and D. M. Lin, "Acquisition through circular correlation by partition for GPS C/A code and P(Y) code," US patent No. 6567042, May 2003.

[5] A. Jovancevic, S. Ganguly, and S. Zigic, "Direct P(Y)/M-code acquisition," in *Proc. ION GNSS*, Long Beach, 2004, pp. 561-572.

[6] D. J. R. V. Nee and A. J. R. M. Coenen, "New fast GPS code acquisition technique using FFT," *Electron. Lett.*, vol. 27, no. 2, pp. 158-160, 1991.

[7] U. Madhow and M. B. Pursley, "Mathematical modeling and performance analysis for a two-stage acquisition scheme for direct-sequence spread-spectrum CDMA," *IEEE Trans. Commun.*, vol. 43, no. 9, pp. 2511-2520, Sept. 1995.

[8] L. Reggiani and G. M. Maggio, "Rapid search methods for code acquisition in UWB impulse radio communications," *IEEE J. Select. Areas Commum.*, vol. 23, no. 5, pp. 898-908, May 2005.

[9] K. M. Chugg and M. zhu, "A new approach to rapid PN code acquisition using iterative message passing techniques," *IEEE J. Select. Areas Commum.*, vol. 23, no. 5, pp. 884-897, May 2005.

[10] C. Yang, M. J. Vasquez, and J. Chaffee, "Fast direct P(Y)-code acquisition using XFAST," in *Proc. ION GPS*, Nashville, TN, 1999, pp. 317-324.

[11] C. Yang, J. Chaffee, J. Abel, and M. J. Vasquez, “Extended replica folding for direct acquisition of GPS P-code and its performance analysis," in *Proc. ION GPS*, Salt Lake City, UT, 2000, pp. 2070-2078.
[12] Y. H. Lee and S. Tantaratana, “Sequential acquisition of PN sequences for DS/SS communications: design and performance," *IEEE J. Select. Areas Commum.*, vol. 10, no. 4, pp. 750-759, May 1992.
[13] Y. H. Lee and S. J. Kim, “Sequence acquisition of DS-CDMA systems employing gold sequences," *IEEE Trans. Veh. Technol.*, vol. 49, no. 6, pp. 2397-2404, Nov. 2000.
[14] J. Ibrahim and R. M. Buehrer, “Two-stage acquisition for UWB in dense multipath," *IEEE J. Select. Areas Commum.*, vol. 24, no. 4, pp. 801-807, Apr. 2006.
[15] H. R. Park, “Performance analysis of a double-dwell serial search technique for cellular CDMA networks in the case of multiple pilot signals," *IEEE Trans. Veh. Technol.*, vol. 48, no. 6, pp. 1849-1830, Nov. 1999.
[16] O.-S. Shin and K. B. Lee, “Differentially coherent combing for double-well code acquisition in DS-CDMA systems," *IEEE Trans. Commun.*, vol. 51, pp. 1046-1050, July 2003.
[17] S. W. Golomb, *Shift Register Sequences*. San Francisco, CA: Holden-Day, 1967.
[18] J. G. Proakis, *Digital Communications*, 3rd ed. New York: McGraw-Hill, 1995.
[19] E. D. Kaplan and C. J. Hegarty (ed.), *Understanding GPS: Principles and Applications*. Norwood, MA: Artech House Publishers, 2006.

Hong Li received the B.S. degree (with honors) in Electronic Engineering and the secondary B.S. degree in Business Administration, both from Sichuan University, Chengdu, China, and both in 2004. He is working toward the Ph.D. degree in Electronic Engineering at Tsinghua University, Beijing, China. His current interests include wireless communications, signal processing, and satellite positioning and navigation.

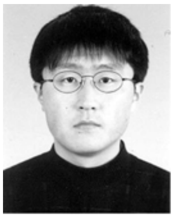

Xiaowei Cui received the B.S. and Ph.D. degrees in Electronic Engineering from Tsinghua University, Beijing, China, in 1999 and 2005, respectively. His research interests include satellite positioning and navigation, information theory and statistical signal processing for wireless communication.

Mingquan Lu received the M.S. degree in Electronic Engineering from the University of Electronic Science and Technology of China, Chengdu, China, in 1993. He jointed the Department of Electronic Engineering of Tsinghua University, Beijing, China, in 2003, and is currently an associate professor and the director of the Institute of High-speed Signal Processing and Network Transmission. His research interests include signal processing, simulation of satellite navigation system, local area navigation system, and software defined receiver.

Zhenming Feng received the B.S. and M.S. degrees in Electronic Engineering from Tsinghua University, Beijing, China, in 1970 and 1981, respectively, both in radar signal processing. He has been with the Department of Electronic Engineering, Tsinghua University, since 1970, where he became a professor in 2000. Before 1990, his research direction was radar signal processing. Now his research interests include broadband access networks, satellite positioning and navigation, and wireless communications.